The Importance of the Petrophysical Properties and External Factors in the Stone Decay on Monuments

Claude Hammecker

PAGEOPH, Vol. 145, No. 2 (1995) 0033-4553/95/020337-25$1.50 + 0.20/0

The Importance of the Petrophysical Properties and External Factors in the Stone Decay on Monuments

CLAUDE HAMMECKER[1,2]

Abstract—In this paper it is proposed to quantify the importance of some physical parameters responsible for stone decay on monuments. The most common decay process is the crystallisation of salt near the surface of the rocks or inside their porous network. Therefore, the water balance in rocks submitted to these special saturation and position conditions has been studied specifically, using the general concepts of water transfer in unsaturated porous media, and using the capillary imbibition kinetics of different rocks. Different parameters have been taken into account for the calculation of the salt crystallisation position: on one hand, several external parameters such as relative humidity, air convection and the presence of solute in solution, and on the other hand, the intrinsic water transfer properties of the rocks. Their relative importance is discussed, considering the potential values that each parameter can reach in nature.

Key words: Salt crystallisation, capillary imbibition kinetics, evaporation, water activity, unsaturated porous media.

1. *Introduction*

The rocks used on buildings are subjected to several types of decay processes (AMOROSO and FASSINA, 1983): physical, chemical, or microbiological, etc. Nevertheless, considering the kinetics and extension of the decay processes of rocks on monuments, it is admitted that the most important factors are physical. Except for the dissolution of carbonate rocks in leached areas, no genuine mineralogical alteration is observed. Rocks are however affected by mechanical desegregation and superficial modifications which are mainly due to frost and salt crystallisation (WINKLER and SINGER, 1972). This paper is especially focused on the study of this latter process, which affects stones in all types of climates. The water balance in stones that determines the crystallisation of salts has been calculated versus different parameters: *external*, such as relative humidity, wind velocity and the presence of

[1] Centre de Géochimie de la Surface (CNRS), 67084 Strasbourg Cedex, France.
[2] Present address: ORSTOM, BP 1386, Dakar, Senegal.

salts in solution, and *internal*, such as the intrinsic water transfer properties of the stones. In this paper only isothermal conditions have been taken into account.

2. General Context

The rocks on monuments often show several types of decay morphologies depending on their petrographical characteristics, on their position on the monument, and on the type of salts involved (JEANNETTE and HAMMECKER, 1993). The most common salt occurrence on monuments, especially in urban areas, is gypsum resulting from the reaction of H_2SO_4 with calcite present either in the rocks or in the surrounding mortars. Gypsum may form superficial black crusts on the surface of stones or it can also lead to contour scaling as it crystallises inside the porous network of the rocks. The crust formation, at least in the first stages, is not damaging to the rock, whereas the crystallisation of gypsum at a few millimetres or sometimes centimetres underneath the surface of the stone, can provoke the breakdown of the external part, which is lightly impregnated with gypsum (ZEHNDER, 1982).

Other types of salts, usually more soluble: halite (NaCl), niter (KNO_3), thenardite (Na_2SO_4), mirabilite ($Na_2SO_4 \cdot 10H_2O$), syngenite ($K_2Ca(SO_4)_2 \cdot H_2O$), etc., are also commonly found on monuments (ARNOLD, 1976). They form salt efflorescence on the surface of the stone such as the niter crystals which frequently cover the walls in cellars, or they may also develop efflorescence on previous superficial gypsum crusts. However these kinds of salts can also be associated with desegregation and alveolization of stone on monuments (HAMMECKER and JEANNETTE, 1988). In the lower part of buildings, submitted to capillary rise of water, soluble salts sometimes crystallise in the porous network of the stones, provoking internal stress and desegregation.

The description of these decay mechanisms can be simplified by considering two extreme conditions: either salts crystallise on the surface of the rocks, without really damaging them, or they crystallise in the rocks causing actual decay (AMOROSO and FASSINA, 1983; JEANNETTE and HAMMECKER, 1992). As the position of salts crystallisation is governed by water balance in rocks, this study centres more specifically on the water transfer processes in unsaturated porous media.

3. Water Transfer Processes

Two different conditions are usually observed for the transfer of water through the rocks on monuments: 1—alternate imbibition and drying in rain-exposed positions on monuments, 2—simultaneous water supply by capillary imbibition and loss by evaporation (steady state, wick condition), in the lower part of the buildings submitted to capillary rise (HAMMECKER, 1993).

3.1 Experiments

Capillary imbibition, and evaporation kinetics can be measured experimentally on rock samples. Usually cylindrical cores of 4 cm in diameter and 10 to 15 cm in height are used for these experiments.

3.1.1 Capillary imbibition kinetics

The previous oven-dried (60°C) rock samples are placed on a thick wet filter paper, providing a continuous and regular water supply. This apparatus is enclosed in a tight container in order to prevent evaporation.

The height of the wetted fringe and the weight of the sample are recorded for increasing time intervals. When plotted versus the square root of time, both show a linear evolution (Figure 1a). Hence two kinetic parameters can be measured:

$$\begin{cases} \mathscr{A}_{[\mathrm{kg}/(\sqrt{\mathrm{s}}\cdot \mathrm{m}^2)]} = W/(S\cdot\sqrt{t}) \\ \mathscr{B}_{[\mathrm{m}/(\sqrt{\mathrm{s}})]} = L/\sqrt{t}. \end{cases}$$

For homogeneous porous media: $\mathscr{A}/(\mathscr{B}\cdot\rho) = N_t$, where N_t is the porosity freely invaded by capillary imbibition, and ρ the fluid density (kg/m^3). Nevertheless these kinetic parameters can be defined as easily, only if the effect of gravity is negligible: with very fine pores or for low capillary rise distances or in the case of horizontal capillary flow. Considering the conditions of stone decay on monuments, in this paper gravity has been neglected. Moreover, in this paper $\mathscr{B}$ is expressed in cm/$\sqrt{h}$ for convenience despite being used in SI unit in the calculations (SI = [cm $\cdot$ $h^{-1/2}$]/6000).

3.1.2 Evaporation kinetics

Water-saturated rock samples are wrapped in polyethylene sheath with an open and regular surface, through which evaporation is allowed. The samples are placed in closed containers where saturated brines control the relative humidity (ACHESON, 1963; SCHLÜNDER, 1963; WYLIE, 1963). Thereafter the weight is recorded regularly. As shown in Figure 1b, two stages with different kinetics can be observed. The first stage of drying, corresponding to the superficial evaporation of water, is linear versus time. Water is drawn by capillary forces from the inner parts of the porous network toward the surface (PEARSE *et al.*, 1949; HALLAIRE and HENIN, 1958). A constant rate of evaporation can be measured:

$$q_{ct} = \frac{W/S}{t} = q_v\cdot\rho, \tag{1}$$

where q_v is the volumic flow rate. When the first stage of drying ends, the critical water saturation is reached θ_c at $t = t(\theta_c)$.

The second stage of drying, with a much slower rate of evaporation, corresponds to the diffusion of water vapour inside the porous network toward the surface. Liquid water is immobile during this stage of drying because pendular saturation has been reached or because the capillary pressures are not high enough to pull water at the surface (PEARSE *et al.*, 1949; BOND and WILLIS, 1969). The rate

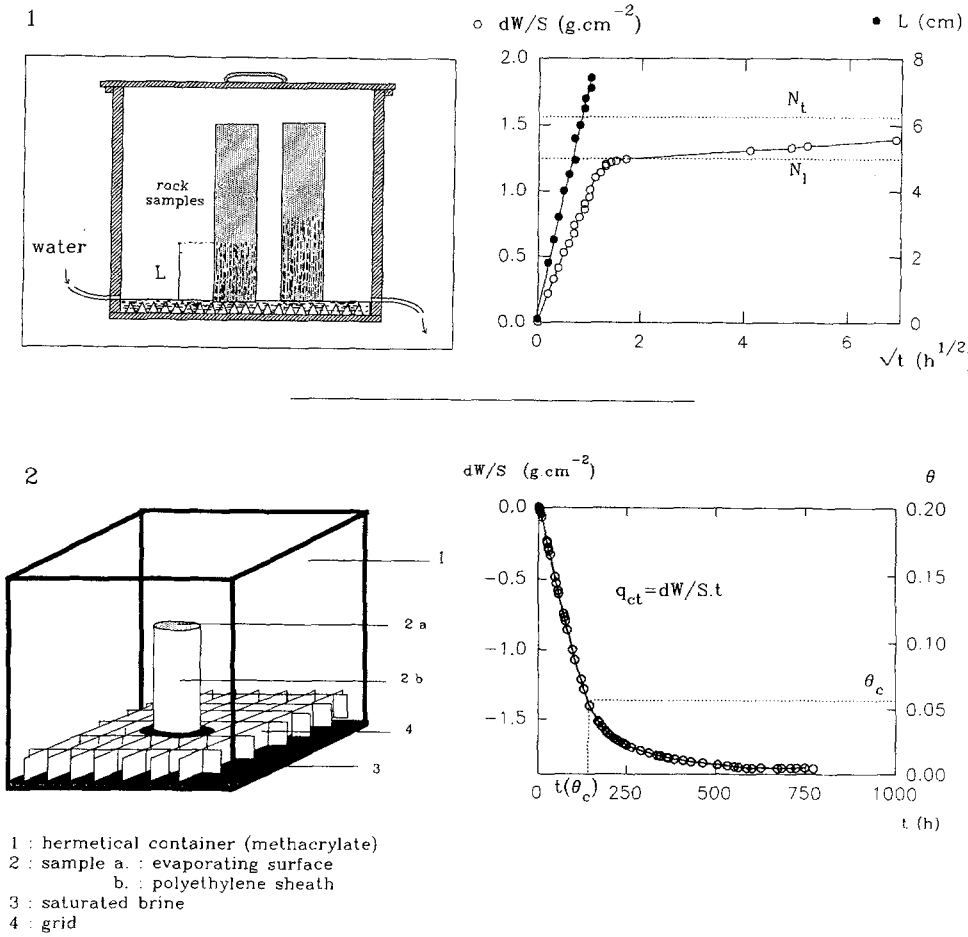

Figure 1
Capillary imbibition: **1a** experiment and **1b** curve, Evaporation: **2a** experiment and **2b** curve.

of this stage of drying depends on the square root of time

$$\Delta W/S = q^* \cdot \sqrt{(t - t(\theta_c))}. \tag{2}$$

In the case of stone degradation on monuments, the most favourable case is reached when the major part of the porous volume is desaturated by superficial evaporation ($\theta_c \to 0$). Hence if salt crystallisation occurs, it mainly takes place on the surface of the rock, without damaging its coherence.

3.2 Transfer in Unsaturated Porous Media

Water transfer in unsaturated conditions is governed by both the relative permeability (or hydraulic conductivity) $K(\psi)$ and the matrix potential ψ, referring

to capillary pressure and gravitational components. The flow is described by the generalised Darcy law

$$\mathbf{q} = -K(\psi)\nabla\psi \tag{3}$$

in one direction (x)

$$q = -K(\psi)\frac{d\psi}{dx} \tag{4}$$

mass conservation expressed in the continuity law, determines the evolution of the water content θ:

$$\frac{\partial\theta}{\partial t} = -\frac{\partial q_x}{\partial x} \tag{5}$$

$$\frac{\partial\theta}{\partial t} = \frac{\partial}{\partial x}\left(K(\psi)\frac{d\psi}{dx}\right). \tag{6}$$

The introdution of the diffusivity $D(\theta) = K(\theta)\cdot(d\psi/d\theta)$ simplifies the mathematical treatment of the equations (4) and (6) for unsaturated flow (CHILDS and COLLIS-GEORGE, 1950):

$$q = -D(\theta)\frac{\partial\theta}{\partial x} \tag{7}$$

$$\frac{\partial\theta}{\partial t} = -D(\theta)\frac{\partial^2\theta}{\partial x^2}. \tag{8}$$

The solution for this diffusion-like flow equation can either be calculated numerically or semi-analytical solutions are proposed for given initial and limit conditions. Diffusivity is usually expressed by the empirical relation of GARDNER and MAYHUGH (1958):

$$D(\theta) = D_i \exp(\beta(\theta - \theta_i)) = D_a \exp(\beta(\theta_a - \theta)), \tag{9}$$

where D_i is the diffusivity for the initial water content θ_i, D_a the diffusivity for air-dry water content θ_a, and β an empirical constant. The water content profile can be calculated at any moment during the drying of a rock sample. Nevertheless, the most important moment occurs when superficial evaporation ceases and the critical water content is reached. GARDNER and HILLEL (1962), give an approximate analytical solution for this case. The following initial and limit conditions must be respected during the first stage of drying:

$$\begin{aligned} \theta &= \theta_i, \quad x > 0, \quad t = 0 \quad \text{(a)} \\ \partial\theta/\partial x &= 0, \quad x = L, \quad r > 0 \quad \text{(b)} \\ D\,\partial\theta/\partial x &= q_v, \quad x = 0, \quad t > 0 \quad \text{(c)}. \end{aligned} \tag{10}$$

For a core with a length L:

$$\frac{\partial\theta}{\partial t} = -\frac{q_v}{L}. \tag{11}$$

Taking into account the conditions (a), (b) and (c), and deriving twice, the following equation is obtained:

$$\theta(x) = \theta_a + \frac{1}{\beta}\ln\left(1 + \frac{q_v \cdot \beta}{D_i} \cdot \left(x - \frac{x^2}{2 \cdot L}\right)\right). \tag{12}$$

The duration of the first stage of drying can be calculated from the average water content $\bar{\theta}$ (SWARTZENDRUBER, 1969):

$$t(\theta_c) = \frac{1}{q_v} \cdot (\theta_i - \bar{\theta}) \tag{13}$$

$$\bar{\theta} = \theta_c = -2 \cdot \beta + \frac{b_2}{\beta} \cdot \ln\left(\frac{b_2 + 1}{b_2 - 1}\right) \tag{14}$$

with

$$b_2 = \sqrt{(b_1 + 1)/b_1}$$

$$b_1 = \beta \cdot L \cdot q_v/(2 \cdot D_i).$$

The evolution of the different parameters governing the superficial evaporation of water such as the data related to diffusivity (D_i and β) and the external rate of evaporation (q_v), is shown in Figure 2.

3.3 Simultaneous Evaporation and Water Supply

In the case of wick-like water transfer conditions, the steady-state equilibrium is reached when capillary imbibition flow is equal to the evaporation flow. As the critical position for salt crystallisation is the surface ($z = 0$) it is important to know the total water balance Q at this position

$$Q_{(0,t)} = q_c - q_e, \tag{15}$$

which is the algebraic sum of the capillary imbibition (q_c) and the evaporation (q_e) flows.

3.3.1 Capillary imbibition

Taking the cylindrical tube model described by the WASHBURN law (1921), the imbibition kinetics can be calculated versus a hypothetical hydraulic radius

$$y = \sqrt{\frac{r \cdot \gamma}{2 \cdot \eta} \cdot t + y_0^2}, \tag{16}$$

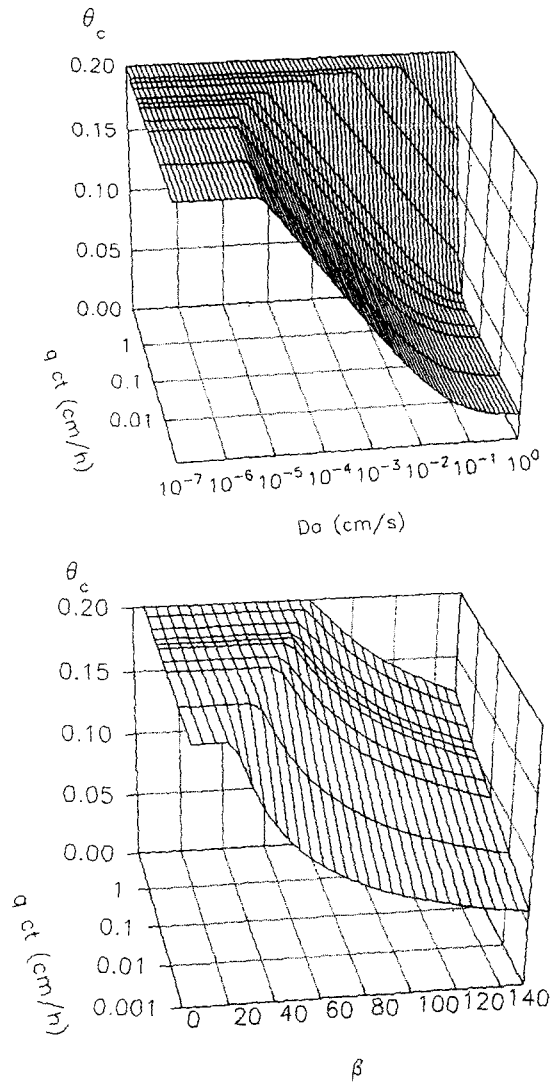

Figure 2
Evolution of the critical water content θ_c versus external (q_{ct}) and internal parameters (D_o and β).

where

γ: surface tension (0.072 N/m for water at 25°C),
η: viscosity ($1.019 \cdot 10^{-3}$ PI for water at 25°C),
y_0: height of the meniscus at $t = 0$.

When the initial height of the meniscus y_0 is equal to 0, the migration of the meniscus in the tube can be formulated as a simple square root of time function

$$y = \mathscr{C} \cdot \sqrt{t}, \tag{17}$$

where $\mathscr{C}$ is equivalent to the experimental $\mathscr{B}$ kinetic parameter. Hence the capillary imbibition flow is

$$q_c = \rho \cdot \frac{dy}{dt} = \rho \cdot \frac{\mathscr{B}^2}{2 \cdot y}. \tag{18}$$

3.3.2 Evaporation

Considering a cylindrical tube partially filled with water, the evaporation flow can be expressed as a function of: the isothermal rate of diffusion for water vapour in pure air $\mathscr{D}$, the difference in water vapour concentration between air near the water and the bulk air volume outside the tube $(c_0 - c_1)$, and the distance between the meniscus and the tube end h:

$$q_e = -\mathscr{D} \cdot \frac{c_0 - c_1}{h}. \tag{19}$$

Nevertheless this relation deriving from FICK's first law, cannot apply directly to diffusion in a mixture of air and water vapour. DE GROOT and MAZUR (1962) introduced a mixing term in equation (19) and expressed it as a function of partial water vapour pressure

$$q_e = -\mathscr{D} \frac{M}{R \cdot T} \frac{P_r}{(P - p_1)} \frac{dp}{dx}, \tag{20}$$

where P is the atmospheric pressure, P_r the reference pressure ($1.013 \cdot 10{-}5$ Pa), p_1 the fixed water vapour pressure, M the molecular mass of water ($1.8 \cdot 10^{-2}$ kg/mol), R the universal gas constant, and T (K) the temperature. For simplification

$$q_e = k \cdot \frac{p_0 - p_1}{h}. \tag{21}$$

DE VRIES and KRUGER (1967) give an empirical relation for k which in SI units is

$$k_{[s]} = -2.17 \cdot 10^{-5} \frac{1.013 \cdot 10^{-5}}{(P - p_1)} \frac{M}{R \cdot T} \left(\frac{T}{273.15} \right)^{1.88}. \tag{22}$$

In order to avoid the indetermination of equations (19) and (21) when: $\lim_{h \to 0} q_e = \infty$, a supplemental parameter depending on air convection ε must be added (JOUANY, 1981):

$$q_e = k \cdot \frac{p_0 - p_1}{h + \varepsilon}. \tag{23}$$

The value of ε is obtained experimentally by measuring the evaporation flow on the free water surface ($h = 0$), submitted to the same evaporating conditions $(k, p_0 - p_1)$. Hence ε represents the thickness of the layer of air over the water surface, in which $p_1 < p < p_0$ (Figure 3). When air convection increases, ε decreases.

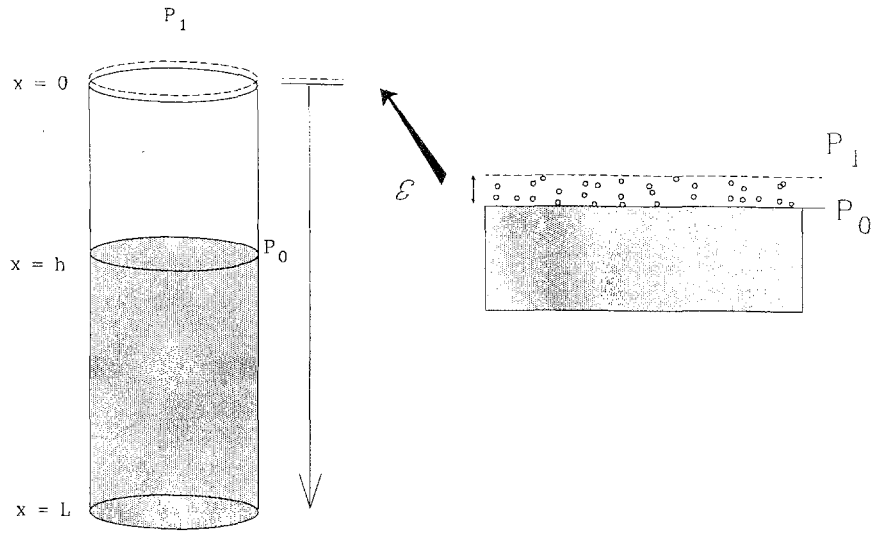

Figure 3
Tube model for evaporation. L: length of the tube, h: distance from the opening, p_0: vapour pressure over the water surface, p_1: vapour pressure in air, ε: distance from the water surface where $p = p_1$.

In a cylindrical tube the evaporation flux is also

$$q_e = \frac{dx}{dt} \cdot \rho, \tag{24}$$

where ρ is the water density. Hence

$$(x + \varepsilon) \cdot dx = \frac{k \cdot (p_0 - p_1)}{\rho} \cdot dt \tag{25}$$

$$\Rightarrow \int_{x_0}^{h} (x + \varepsilon) \cdot dx = \tfrac{1}{2} \cdot (h^2 - x_0^2) + \varepsilon \cdot h + \varepsilon \cdot h + \varepsilon \cdot x_0 = \frac{k \cdot (p_0 - p_1)}{\rho} \cdot (t - t_0).$$

In this case, only the positive solution of this second-order equation, is considered

$$h = -\varepsilon + \sqrt{x_0^2 + \varepsilon^2 + \frac{2 \cdot k \cdot (p_0 - p_1)}{\rho} \cdot (t - t_0)}, \tag{26}$$

where x_0 is the initial height of the meniscus. When air convection is important, ε can be neglected, hence the kinetic of migration of the meniscus is the function of the square root of time. This phenomenon is then comparable to the kinetic of the second stage of drying of rocks (q^*).

3.3.3 Water balance

Although the structure of the porous media in rocks cannot be compared to cylindrical tubes, the imbibition and evaporation kinetics are similar and easily

calculated with this model. The steady-state equilibrium is reached for

$$q_c = q_e \tag{27}$$

$$\Rightarrow \quad \rho \cdot \frac{\mathscr{B}^2}{2 \cdot y} = k \cdot \frac{(p_0 - p_1)}{L + \varepsilon - y}. \tag{28}$$

The equilibrium position is

$$y_{\text{eq}} = \frac{(L + \varepsilon) \cdot \mathscr{B}^2 \cdot \rho}{2 \cdot k \cdot (p_0 - p_1) + (\mathscr{B}^2 \cdot \rho)}. \tag{29}$$

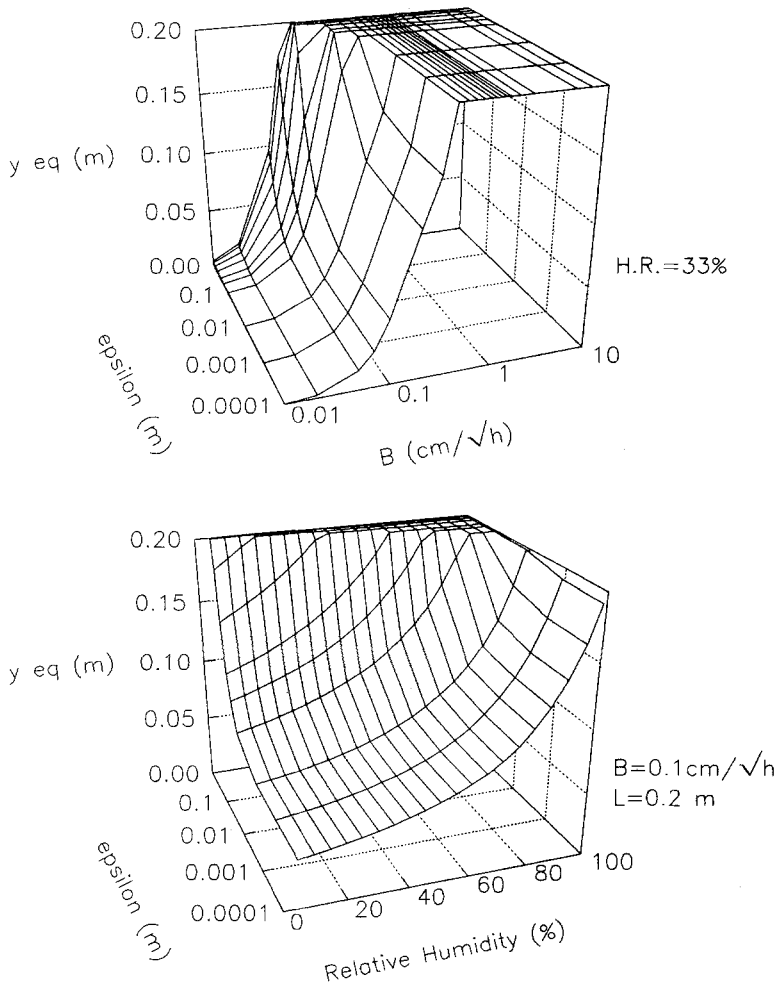

Figure 4
Evolution of the equilibrium height in wick-like conditions.

In Figure 4 the evolution of equilibrium height y_{eq} is plotted versus different parameters, such as the capillary imbibition kinetic $\mathscr{B}$, the "wind velocity" ε, the relative humidity p/p_0 and the length of the capillary tube L.

4. *The Presence of Salts*

In nature, and especially on monuments, the rocks do not contain distilled water but rather solutions which form brines by concentrating under evaporation and finally form salts. The presence of ions, especially near the surface where they are concentrated by the evaporation of water, may influence the water activity a_w. As the evaporation rate depends on the partial water vapour pressure gradient, the modification of the water activity and the partial vapour pressure just above the water surface will alter the water balance in the rock:

$$q_{ev} = k \cdot \frac{p_0^* - p_1}{h}, \tag{30}$$

where $p_0^* = a_w \cdot p_0$. The evolution of water activity depends on the concentration and the type of ions. In order to calculate the water activity in the presence of ions, the ionic interaction model of PITZER (1973, 1979) has been chosen, rather than DEBYE-HUCKEL's model (1923), because of the high ionic strengths in the brines ($I > 1$), which are necessary for the crystallisation of the previously mentioned soluble salts. Hence for a given type of salt and molality the water activity can be calculated (Appendices A1 and A2). Nevertheless the main problem is the calculation of the evolution of the ion concentration at the air-solution interface. In order to solve this problem two cases have been taken into account:

No chemical diffusion: Considering that the diffusion of ions in solution is slow compared to water transfer processes, space under the meniscus has been divided into layers of determined thickness λ (Fig. 5a). In this study an arbitrary thickness of 10 μm has been chosen, because it represents the main salt-crystal size observed on monuments. When 10 μm of water at the top of the meniscus evaporates, the ions remain in the water layer previously situated underneath. Hence concentration in the upper layer situated underneath the meniscus evolves as follows:

$$\left.\begin{array}{ll} t_0, & C_0 \\ t_1, & C_1 = 2 \cdot C_0 \\ t_n, & C_n = n \cdot C_0 \end{array}\right\} \Rightarrow \quad C(t) = C_0 \cdot (1 + h(t)/\lambda). \tag{31}$$

Instant chemical diffusion: Ions are immediately distributed over the entire volume of water so concentration is kept homogeneous in the

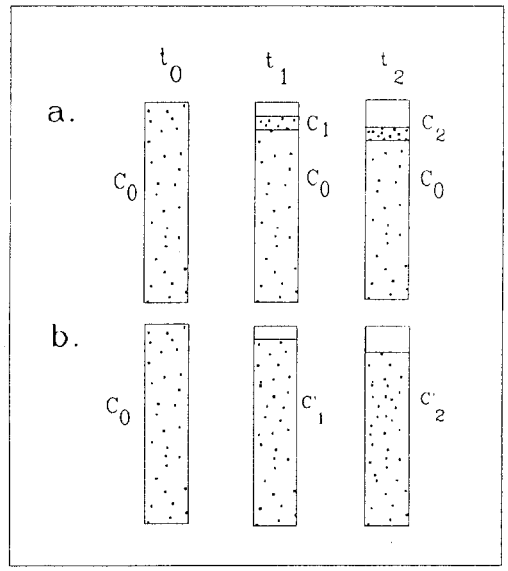

Figure 5
Chemical diffusion models: **1.** instant diffusion, **2.** no diffusion.

tube (Fig. 5b):

$$C(t_0) = \frac{V(t_{j-1}) \cdot C(t_{j-1})}{V(t_{j-1}) - q_{\text{ev}} \cdot t}, \tag{32}$$

where $V(t_j) = V(t_{j-1}) + (q_{\text{cap}} - q_{\text{ev}}) \cdot t$.

To solve this system, numerical resolution has been used in order to relate the height of the meniscus in the tube, the global flow, and the concentration. Equilibrium height is obtained by incrementing dx, calculated from the capillary imbibition and evaporating flux at each new position x and new concentration, hence p_0^*:

$$dy = dy_{\text{cap}} - dy_{ev} = \left(\frac{\mathscr{B}^2}{2 \cdot y} + k \frac{p_0^* - p_1}{\rho \cdot (L + \varepsilon - y)} \right) \cdot dt \tag{33}$$

$$\Rightarrow \quad y(dt_2) = y(dt_1) + dy_1. \tag{34}$$

To perform this calculation, a small increment of time ($dt = 100$ s) has been chosen.

In order to simplify the calculation, only aqueous solutions of some binary salts have been tested. Nevertheless these salts have been chosen for their possibility to crystallise in rocks on monuments, and in order to cover a wide range of water activity in the corresponding saturated brines (Appendix A3).

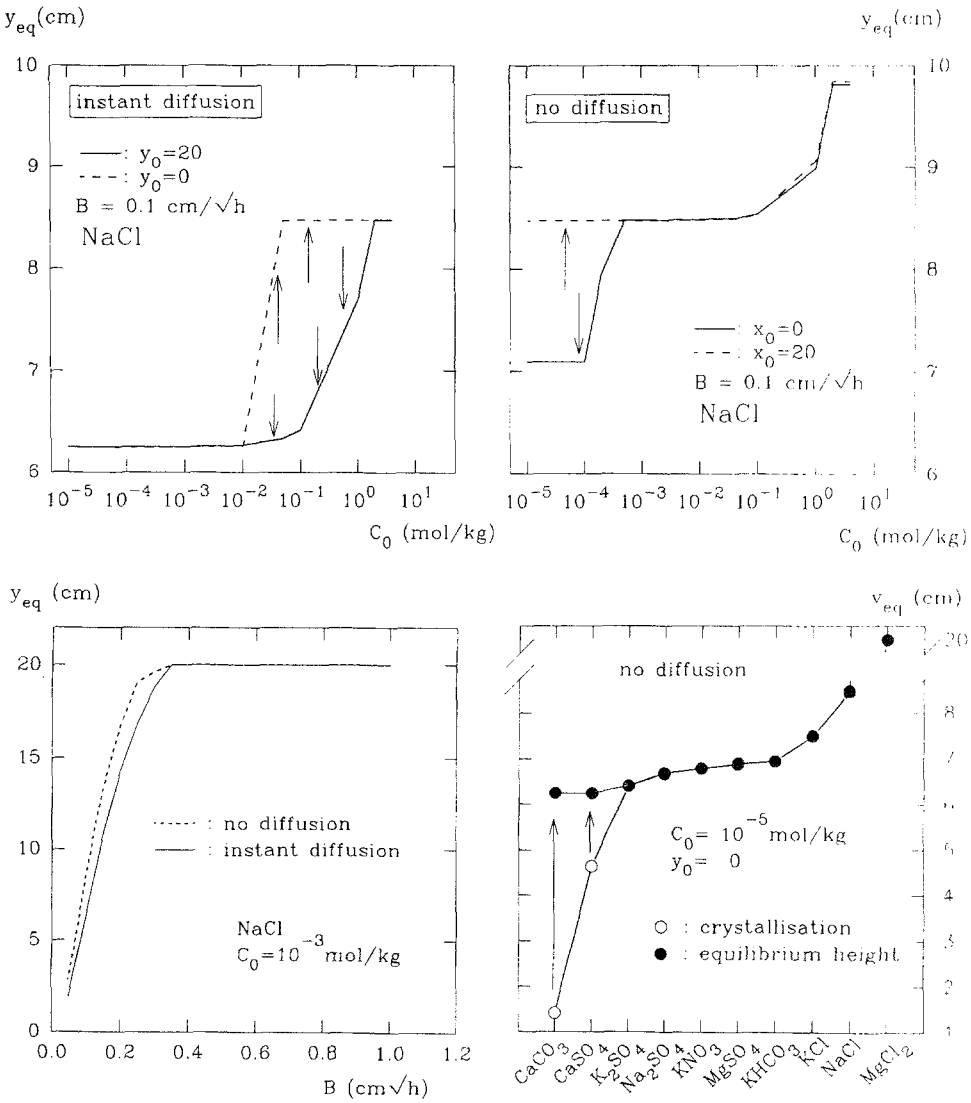

Figure 6
Evolution of equilibrium height taking into account the presence of salt.

The results displayed in Figure 6 can be described as follows:

- as the concentration of the solution near the interface evolves faster with the *no chemical diffusion model* than with the *instant chemical diffusion model*, the calculated equilibrium heights h_{eq} are slightly higher with the first model than with the latter. Nevertheless both models converge toward the same tendencies.
- The initial concentration of the solution C_0 is an important factor governing the equilibrium height: an aqueous solution with a high concentration pro-

motes the hydrodynamical equilibrium position to be nearer the surface than with a dilute solution.

- Equilibrium height depends on the initial position of the meniscus: in these chosen conditions, for upward flow ($x_0 = 0$ cm), h_{eq} is higher than for the downward flow ($x_0 = 20$ cm).
- The influence of the most soluble salts such as NaCl, $Na_2SO_4 \cdot 10H_2O$ or KCl is considerably more important than for less soluble salts like $CaCO_3$ or $CaSO_2 \cdot 2H_2O$.
- The influence of the capillary imbibition kinetic is predominant over the other parameters because moderate variations for $\mathscr{B}$ lead to important variations for h_{eq}.

5. Discussion

5.1 The Models

It must be borne in mind that the mathematical models used for this study are based on several assumptions constraining their application. The concept of diffusivity in the CHILDS and COLLIS-GEORGE equation assumes an initial uniform water profile in the stone which implies a homogeneous nonstratified porous medium. Moreover, the use of diffusivity is valid only in nonhysteretic porous media free of any temperature gradient (HILLEL, 1971). These conditions are realised with the sample in the laboratory where water profile, sample homogeneity and internal temperature gradient are precisely controlled. In the case of hysteretic rock samples, as only evaporation is considered, diffusivity is calculated by taking into account the drainage branch of the hysteresis in the capillary pressure curve ($\psi - \theta$). The CHILDS and COLLIS-GEORGE equation is validated for these conditions for which the importance of elemental external parameters has been tested. As the purpose of this study is to quantify the influence of some internal and external parameters on the water transfer processes governing the rock decay, and not to describe the entire and complex system of rocks on monuments, the use of these equations is justified.

On the other hand, the validity of the WASHBURN equation (16) is restrained to the capillary imbibition into straight cylindrical tubes. Obviously, the geometry of the porous network in natural rocks is dissimilar to this simple model. However, based on this equation, some authors extended its application to less monotonous pore shapes (SZEKELY *et al.*, 1971; DULLIEN, 1979; LEVINE, *et al.*, 1980; HAMMECKER *et al.*, 1993). In any case, the capillary imbibition kinetic described by these models and the experimental data, are similar to the Washburn equation, despite the hydraulic radius (r) in the latter having no physical reality. Hence, for this study, based on water transfer processes, the use of this equation is satisfactory.

5.2 The Results

Many parameters govern the water balance in rocks and consequently the position of potential salt crystallisation. However, considering that this entire study has been performed in ideal isothermal conditions, the most influential external parameter is certainly the air convection or *wind velocity* formulated by ε whereas relative humidity has less important effects.

Nevertheless, it is clear that in the case of simple drying, the internal parameters related to the diffusivity such as D_i and β, are more important in determining the critical water content θ_c than the external rate of evaporation (q_{cl}). Considering that some of the highest potential evaporation rates measured in arid inhabited areas (Agadez, Niger), are about 2.4 cm/day (BRUNEL and BOURON, 1992), their influence on critical water content are negligible compared to the diffusivity. On the other hand, the potential range of diffusivity for different rocks used on monuments is very wide. The results shown in Table 1 for some common sedimentary rocks used on monuments are very explicit, because their diffusivity (D_a and D_i) are seen to range over four orders of magnitude. More generally their petrophysical properties, can show severe differences. Despite the average grain size varying widely (20–750 μm), it is not a determining factor for the petrophysical properties such as porosity (N_t), saturated hydraulic conductivity (K_0), or capillary kinetic imbibition. The coarsest rock (Gueberschwihr sandstone) is at the same time the less porous and the less permeable, whereas the finest rock (Laspra limestone) is more porous and 1000 times more permeable than the former. The important secondary silicification features present in the Gueberschwihr sandstone are responsible for these petrophysical parameters. As observed on the mercury porosimetry curves (Fig. 7),

Table 1

Examples of petrophysical properties and diffusivity values in some sedimentary rocks

Rock	Darney sandstone	Gueberschwihr sandstone	Laspra limestone	Hontoria limestone
Petrography	Coarse sandstone clayey coating	Coarse sandstone highly silicified	Fine homogeneous dolomicrit	Coarse heterogeneous bioclastic limestone
$\overline{GS}$ (μm)	250	450–750	20	250
N_t (%)	25	6	32	20
K_0 (m · s^{-1})	$2.4 \cdot 10^{-5}$	$6 \cdot 10^{-10}$	$2.4 \cdot 10^{-7}$	$2.4 \cdot 10^{-6}$
S_{sa} (m^2/kg)	$2.53 \cdot 10^3$	$0.27 \cdot 10^3$	$4.6 \cdot 10^3$	$0.8 \cdot 10^3$
D_a (m^2/s)	$1.2 \cdot 10^{-7}$	$6.9 \cdot 10^{-11}$	$5.5 \cdot 10^8$	$4.1 \cdot 10^{-8}$
β	34	156	60	45
D_i (m^2/s)	$2.6 \cdot 10^{-4}$	$2 \cdot 10^{-8}$	$7.2 \cdot 10^{-5}$	$1.4 \cdot 10^{-4}$
θ_c/θ_i (%)	30	83	42	32
$\mathscr{B}$ (cm · $h^{-1/2}$)	5.2	0.3	2.4	7.1

$\overline{GS}$: average grain size

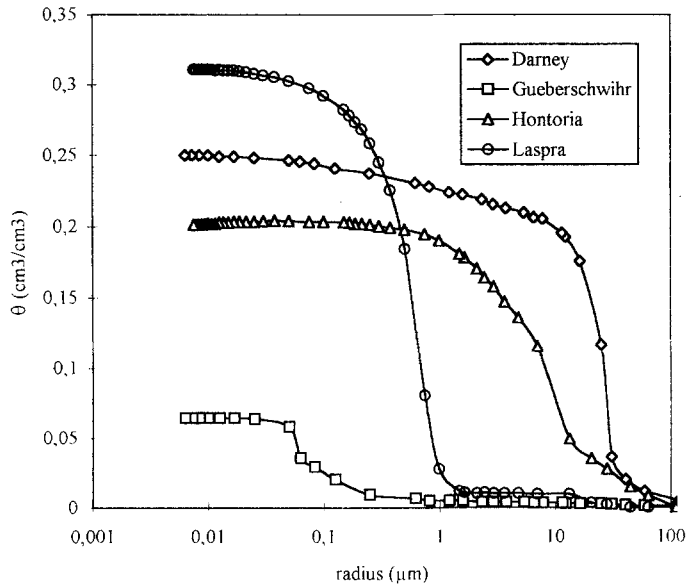

Figure 7
Mercury porosimetry curves.

half of the porous volume of this sandstone is connected through necks narrower than 0.1 μm, whereas in the other rocks, including the micrite, the pore threshold shows far higher interconnection sizes. The saturated hydraulic conductivity and diffusivity values of these rocks are coherent with the corresponding pore size distributions.

For high diffusivity, regardless of the external evaporation conditions, the critical water content ($\theta_c/\theta_i \to 0$) is very low, which means that evaporation preferentially takes place on the surface of the rock. On the other hand, for very low diffusivity, evaporation occurs mainly inside the porous network of the rock ($\theta_c/\theta_i \to 1$). External conditions influence the evaporation of water in a rock only for intermediate diffusivity values.

In the *wick-like conditions*, the influence of the capillary imbibition kinetic $\mathscr{B}$ is predominant, because very slight variations for $\mathscr{B}$ lead to an important alteration in the hydrodynamical equilibrium position (h_{eq}). As shown in Table 1, the variation of this coefficient is also important in sedimentary rocks. It is monitored by the pore size distribution determined by mercury porosimetry. Nevertheless, depending on petrographical features, such as clayey coating, or superficial rugosity on grains, in some cases the specific surface area can provide better information on the capillary imbibition kinetic (HAMMECKER and JEANNETTE, 1995).

Considering the presence of salts in solution, it has been shown, especially for the most soluble ones, that they tend to restrain the evaporation flux q_{ev}, and hence

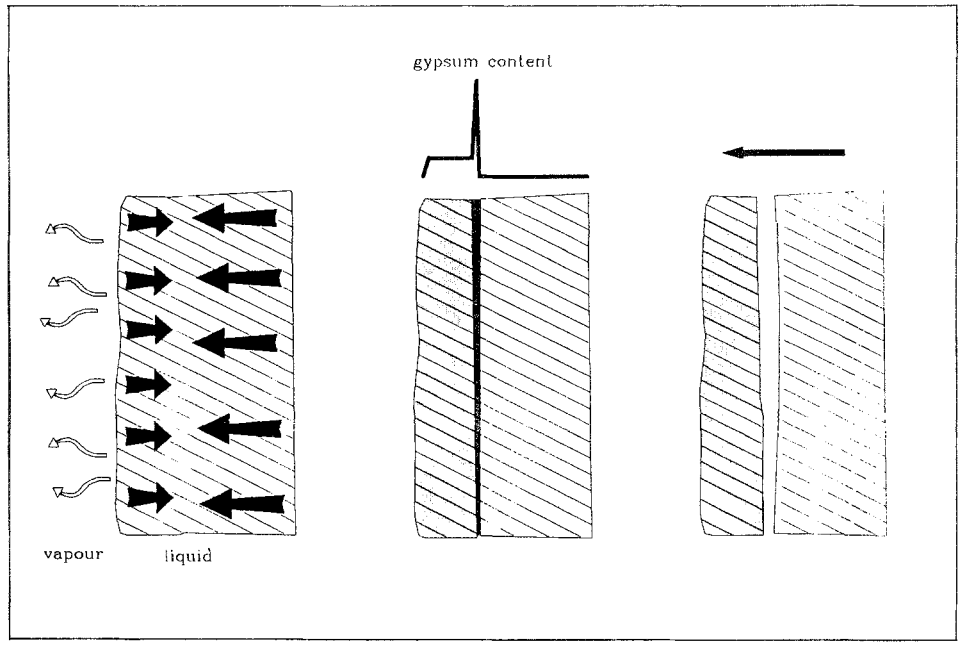

Figure 8
Schematic representation of the formation of contour scaling.

increase the probability of superficial salt crystallisation (b_{eq} is higher). In the case of a low capillary imbibition kinetic ($\mathscr{B}$), the presence of salts for which in the saturated brines the water activity drops under 0.9 (Appendix A.3), the hydrodynamical equilibrium position of the meniscus is raised toward the surface. Hence, sub-superficial salt crystallisation is promoted. On the other hand, for salts such as calcite or gypsum the effect on water activity is negligible, but as their solubilities are very low, they crystallise promptly, before reaching the hydrodynamical equilibrium position. Consequently, while the meniscus is moving from the surface toward the equilibrium position, crystallites of salts are left in the superficial part. This mathematical result can be directly related to the features observed on rocks affected by contour scaling in monuments: the external part of the rock which falls off, is partially impregnated with gypsum, whereas the highest gypsum concentration is observed at the point of the fracture, for which it is responsible (Figure 8).

Nevertheless, for the simple *drying condition and the wick-like condition*, the intrinsic parameters of water transfer in the porous network of the rocks mainly govern the water balances and the position of salt crystallisation. Hence, the potential form and magnitude of the decay of the rock depend basically on the rock's pore structures influencing the water transfer.

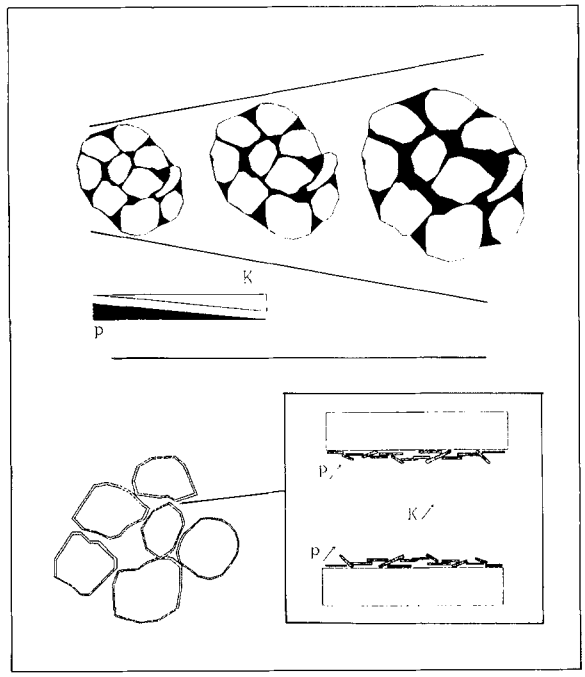

Figure 9
Theoretical porous geometry for high diffusivity: **a.** pore distribution in the rock, **b.** pore structure.

The optimal conditions for rocks used on monuments are those of high diffusivity, which guarantees a significant drainage of the rocks during the superficial stage of evaporation, and those of high capillary imbibition kinetics allowing a positive flux of water at the evaporating surface. An ideal theoretical pore size distribution can be proposed to satisfy these conditions of maximum liquid transfer toward the surface, with three types of pores (Figure 9a) organised in layers parallel to the evaporating surface of the rock:

- *fine driving pores*, situated near or on the evaporating surface of the rock, in which high capillary pressure allows water to drain from internal parts,
- *intermediate conducting pores*, permitting the transfer of water towards the surface with a satisfactory hydraulic conductivity,
- *coarse reservoir pores*, situated inside the rock, with low capillary pressure being easily drained and representing the main porous volume.

This distribution favourable to high diffusivity is also suitable for high capillary imbibition kinetic, as in conical shaped pores, the meniscus accelerates towards the narrowest end (HAMMECKER and JEANNETTE, 1994).

On the other hand, contrary to this theoretical "layered" pore distribution, a natural ideal pore structure, enhancing the probability for superficial evaporation, can be observed. In fact the example of Darney sandstone is very explicit of this

pore structure: its wide pores and interconnections allow a high hydraulic conductivity, whereas at the same time, the superficial roughness on the grains represented by its uniform clayey coating, can be considered as a microporous network (DULLIEN *et al.*, 1989) which is responsible for high capillary pressures, able to drive the water toward the surface (Figure 9b) The coexistence of two parallel porous networks, one macroporous and the other microporous, allows to combine high hydraulic conductivity to high capillary pressure, which are apparently antangonistic properties, in order to achieve important diffusivity.

6. *Conclusion*

The physical decay processes affecting the rocks on monuments, and related to water transfer and associated salt crystallisation, have been studied quantitatively in isothermal conditions. This study has been based on two different approaches. On one hand, traditional water transfer concepts and equations in unsaturated porous media, usually used in soil science, have been adapted to this specific problem. On the other hand, some calculation models have been designed, based on simple capillary and evaporation kinetic measurements. Although the geometry of the porous networks of rocks cannot be compared to cylindrical tubes, their hydrodynamical behaviours are very similar (DULLIEN, 1979; HAMMECKER *et al.*, 1993). Hence the kinetics of these phenomena have been treated as theoretical cylindrical tubes. The physical influence of the presence of solute on the evaporation fluxes has been quantified by introducing the evolution of water activity calculated with the model of PITZER (1973). The most important external factor governing the water transfer in rocks submitted to these conditions, has been determined as being the air convection (wind velocity), whereas the influence of relative humidity is less important. Contrastingly, it has been shown that the presence of solute in solution modifies efficiently the water balance in rocks, especially for those leading to the crystallisation of the most soluble salts (NaCl, Na_2SO_4, KCl, etc.). For calcium sulphate solutions, the effect on water balance is almost negligible, but the mechanism of contour scaling has been demonstrated quantitatively.

Nevertheless, this study shows that the intrinsic parameters of the rocks, diffusivity D and capillary imbibition kinetic coefficient $\mathscr{B}$, are the actual determining factors for the water balance, for the crystallisation position and consequently for the decay forms. In fact when different rocks are submitted to the same environmental conditions on a monument, and they evolve differently, it is regardless of their chemical and mineralogical composition, but rather depends on their petrophysical properties which manage the water transfer (quantities and kinetics).

Finally, an ideal pore structure and an ideal pore distribution have been proposed in order to optimise the diffusivity and the imbibition kinetic, hence to promote the transfer of liquid water toward the surface of the rock.

Appendix A.1

Calculation of the water activity a_w:

$$a_w = \exp\left(-\frac{\phi}{55.51} \cdot \sum_j m_j\right)$$

the osmotic coefficient ϕ is calculated with the ion interaction model of PITZER (1973):

$$\sum m_i(\phi - 1) = 2 \cdot \left(-\frac{A^\phi \cdot I^{3/2}}{1 + 1.2I^{1/2}} + \sum_c \sum_a m_c \cdot m_a (B^\phi_{ca} + Z \cdot C_{ca}) + \sum_{c<} \sum_{c'} m_c \cdot m_{c'} \cdot \left(\Phi^\phi_{cc'} + \sum_a m_a \Psi_{cc'a}\right) + \sum_{a<} \sum_{a'} m_a \cdot m_{a'} \left(\Phi^\phi_{aa'} + \sum_c m_c \Psi_{aa'c}\right) + \sum_n \sum_a m_n \cdot m_a \lambda_{na} + \sum_n \sum_c m_n \cdot m_c \lambda_{nc} + \sum_n \sum_c \sum_a m_n \cdot m_c \cdot m_a \cdot \xi_{nca}\right), \tag{35}$$

which for a single binary salt solution becomes:

$$\sum m_i(\phi - 1) = 2 \cdot \left(-\frac{A^\phi \cdot I^{3/2}}{1 + 1.2I^{1/2}} + \sum_c \sum_a m_c \cdot m_a (B^\phi_{ca} + Z \cdot C_{ca})\right), \tag{36}$$

where

A^ϕ: constant equal to 0.391 at 25°C

I: ionic strength: $I = 1/2(\beta^+ \cdot z^{+2} + \beta^- \cdot z^{-2}) \cdot m$
where β^+, β^- and z^+, z^- are respectively the number and charge of the cations and anions
m is the molality

m_c, m_a: molality of cation and anion with respective charges z_c and z_a

B^ϕ_{ca}: coefficient representing the interaction between two ions and their capacity to join
$B^\phi_{ca} = \beta^{(0)}_{ca} + \beta^{(1)}_{ca} \exp(-\alpha \cdot \sqrt{I}) + \beta^{(2)}_{ca} \exp(-12\sqrt{I})$ the coefficients β depend on each salt type and $\alpha = 2$ if $\beta^{(2)} = 0$ or $\alpha = 1.4$ if $\beta^{(2)} \neq 0$

A: sum of the equivalent concentrations $Z = \sum_i |z_i| m_i$

C_{ca}: parameter related to C^ϕ_{ca}: $C_{ca} = C^\phi_{ca}/(2 \cdot \sqrt{|z_c \cdot z_a|})$

Appendix A.2

Coefficients β^0, $\beta^{(1)}$, $\beta^{(2)}$ and C^ϕ, for simple electrolytes (PITZER, 1979).

Cations	Anions	$\beta^{(0)}_{ca}$	$\beta^{(1)}_{ca}$	$\beta^{(2)}_{ca}$	C^ϕ_{ca}
Na	Cl	0.0765	0.2644	—	0.00127
Na	SO_4	0.01958	1.113	—	0.00497
Na	HCO_3	0.0277	0.0411	—	—
Na	CO_3	0.0399	1.389	—	0.00440
Na	NO_3	0.0068	0.1783	—	−0.0072
K	Cl	0.04835	0.2122	—	−0.00084
K	SO_4	0.04995	0.7793	—	—
K	HCO_3	0.0296	−0.013	—	−0.008
K	CO_4	0.1488	1.43	—	−0.0015
K	NO_3	−0.0816	0.0494	—	0.0066
Ca	Cl	0.3159	1.614	—	−0.00034
Ca	SO_4	0.20	3.1973	−54.24	—
Ca	HCO_3	0.4	2.977	—	—
Ca	CO_3	—	—	—	—
Mg	Cl	0.35235	1.6815	—	0.00519
Mg	SO_4	0.2210	3.343	−37.23	0.025
Mg	HCO_3	0.329	0.6072	—	—
Mg	CO_3	—	—	—	—

Appendix A.3

Solubility product (log K) for several binary salts, the corresponding saturation concentration, and water activity in the saturated brine at 25°C and at 1 atm.

Mineral	Formula	log(K)		C_{sat}(mol/kg)	a_w
calcite	$CaCO_3$	−8.41	(1)	$6.75 \cdot 10^{-5}$	0.999998
gypsum	$CaSO_4 \cdot H_2O$	−4.58	(1)	$2.745 \cdot 10^{-2}$	0.99933
arcanite	K_2SO_4	−1.776	(1)	$7.084 \cdot 10^{-1}$	0.9746
mirabilite	$Na_2SO_4 \cdot 10H_2O$	−1.228	(1)	1.93992	0.936
niter	KNO_4	−0.097	(2)	3.99	0.923
epsomite	$MgSO_4 \cdot 7H_2O$	−1.881	(1)	2.999	0.9058
kalcinite	$KHCO_3$	−0.2857	(1)	3.5818	0.90477
sylvite	KCl	0.9	(1)	4.8014	0.8428
halite	NaCl	1.57	(1)	6.1029	0.7545
hexahydrite	$MgCl_2 \cdot 6H_2O$	4.455	(1)	5.7126	0.3435

(1) HARVIE and WEARE (1984)
(2) ROBIE *et al.* (1978)

Appendix A.4

Algorithm for the calculation of the equilibrium height in the *wick-like* conditions, in presence of salt.

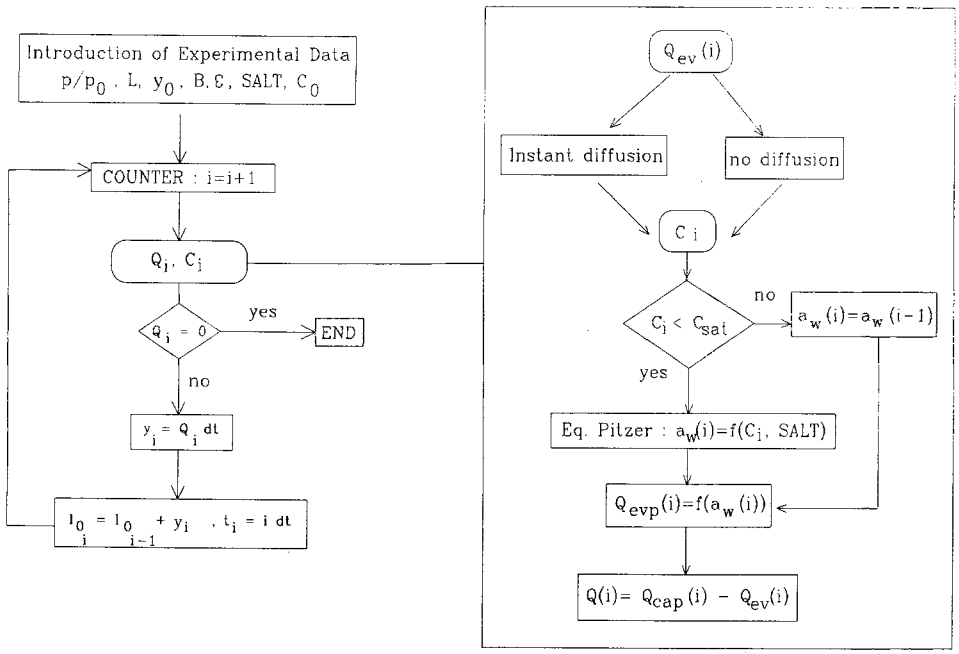

REFERENCES

ACHESON, D. T., *Vapor Pressure of Saturated Aqueous Salt Solutions. Humidity and Moisture* (Rheinhold Publ. Corp., New York 1963) *3*, 521–530.

AMOROSO, G. G., and FASSINA, V. (1983), *Stone Decay and Conservation*, Materials Science Monograph *11*, Elsevier, 453 pp.

ARNOLD, A. (1976), *Behaviour of Some Soluble Salts in Stone Deterioration*, 2nd Internat. Symp. on the Deterioration of Building Stones, Athens, 27–36.

BOND, J. J., and WILLIS, W. O. (1969), *Soil Water Evaporation: Surface Residue Rate and Placement Effects*, Soil Sci. Soc. Am. Proc. *33*, 445–448.

BRUNEL, J. P., and BOURON, B. (1992), *Evaporation des nappes d'eau libres en Afrique Sahelienne et Tropicale*, Document CIEH-ORSTOM, Oct. 1992, 402 pp.

CHILDS, E. C., and COLLIS-GEORGE, N. (1950), *The Permeability of Porous Materials*, Proc. Roy. Soc. *201A*, 392–405.

DEBYE, P., and HUCKEL, E. (1923), *Zur Theorie der Electrolyte*, Phys. Z. *24*, 185–208.

DEBYE, P., and HUCKEL, E. (1923), *Zur Theorie der Electrolyte*, Phys. Z. *24*, 305–325.

DULLIEN, F. A. L., *Porous Media—Fluid Transport and Pore Structure* (Academic Press, New York 1979) 396 pp.

DULLIEN, F. A. L., ZARCONE, C., MACDONALD, I. F., COLLINS, A., and BOCHARD, R. D. E. (1988), *The Effects of Surface Roughness on the Capillary Pressure Curves and the Heights of Capillary Rise in Glass Bead Packs*, J. Colloid and Interface Sci. *127* (2), 362–372.

GARDNER, W. R. and MAYHUGH, M. S. (1958), *Solutions and Tests of the Diffusion Equation for the Movement of Water in Soil*, Soil Sci. Soc. Am. Proc. *22*, 197–201.

GARDNER, W. R., and HILLEL, D. L. (1962), *The Relation of External Evaporative Conditions to the Drying of Soils*, J. Geophys. Res. *67* (11), 4319–4325.

DE GROOT, S. R., and MAZUR, P., *Nonequilibrium Thermodynamics* (North-Holland Publ. Co., Amsterdam 1962).

HALLAIRE, M., and HENIN, S. (1958), *Dessèchement du sol et évolution des profils hydriques*, C. R. Acad. Sci. *46*, 2151–2153.

HAMMECKER, C., and JEANNETTE, D. (1988), *Rôle des propriété physiques dans l'altération de roches carbonatées: Exemple de la façade ouest de Notre-Dame-La Grande de Poitiers (France)*, Proc. VIth Int. Cong. on Deterioration and Conservation of Stone, Toruń (Poland), 266–275.

HAMMECKER, C., (1993), *Importance des transferts d'eau dans la dégradation des pierres en oeuvre*, Ph.D. Thesis, Université Louis Pasteur, Strasbourg.

HAMMECKER, C., MERTZ, J. D., FISCHER, C., and JEANNETTE, D. (1993), *A Geometrical Model for Numerical Simulation of Capillary Imbibition in Sedimentary Rocks*, Transport in Porous Media *12* (3), 125–141.

HAMMECKER, C., and JEANNETTE, D. (1994), *Modelling the Capillary Imbibition in Sedimentary Rocks: Role of Petrographical Features*, Transport in Porous Media *17* (3), 285–303.

HARVIE, C. E., and WEARE, J. H. (1980), *The Prediction of Mineral Solubilities in Natural Waters: The $Na-K-MG-Ca-Cl-SO_4-H_2O$ System from Zero to High Concentration at 25°C*, Geochim. Cosmochim. Acta *44*, 981–997.

HILLEL, D., *Soil and Water — Physical Principles and Processes* (Adacemic Press, Inc., Orlando 1971) 299 pp.

JOUANY, C. (1981), *Transfert d'eau par évaporation dans les milieux argileux*, Ph.D. Thesis, Université Paul Sabatier, Toulouse, 102 pp.

JEANNETTE, D., and HAMMECKER, C., *Facteurs et mécanismes des altérations*. In *La conservation de la pierre monumentale en France* (Presses du CNRS 1992) pp. 73–81.

JEANNETTE, D., and HAMMECKER, C. (1993), *Importance des structures de porosité dans l'altération des pierres des monuments*, Coll. Sédimentologie et Géochimie de la Surface, à la Mém. de G. Millot, Les Coll. de L'Acad. des Sci. et Cadas., 307–319.

LEVINE, S., LOWNDES, J., and REED, P. (1980), *Two Phase-fluid Flow and Hysteresis in a Periodic Capillary Tube*, J. Colloid. Interface Sci. *77*, 253–263.

PEARSE, J. F., OLIVER, T. R., and NEWITT, D. M. (1949), *The Mechanisms of Drying of Solids: I. The Forces giving Rise to Movement of Water in Granular Beds during Drying*, Trans. Inst. Chem. Eng., London *27*, 1–8.

PITZER, K. S. (1973), *Thermodynamics of Electrolytes I: Theoretical Basis and General Equations*, J. Phys. Chem. *77*, 268–2777.

PITZER, K. S., *Theory: Ion interaction approach*. In *Activity Coefficients in Electrolyte Solutions*, 1 (ed. Pytkowicz, R. M.) (CRC Press 1979) *77*, 157–208.

ROBIE, R., HEMINGWAY, B., and FISCHER, J. (1978), *Thermodynamic Properties of Minerals and Related Substances at 298.15°K and 1 bar (10^5 Pascals) Pressure and at Higher Temperatures*, U.S. Geol. Surv. Bull. *1452*, 456 pp.

SCHÜNDER, E. U., *A simple procedure for measurement of vapor pressure over aqueous salt solutions* — In Humidity and Moisture (Rheinhold Publ. Corp., New York 1963) *3*, pp. 535–544.

SWARTZENDRUBER, D., *The flow of water in unsaturated soils*. In *Flow Through Porous Media* (ed. De Wiest) (Academic Press, New York 1969) pp. 215–292.

SZEKELY, J., NEUMANN, A. W., and CHUANG, Y. K. (1971), *The Rate of Capillary Penetration and the Applicability of the Washburn Equation*, J. Colloid Interface Sci. *35*, 273–283.

DE VRIES, D. A., and KRUGER, A. J. (1967), *On the value of diffusion coefficient of water vapour in air*. In *Phénomènes de transport avec changement de phase dans les milieux poreux colloïdaux*, Ed. CNRS, *160*, 61–72.

WASHBURN, E. W. (1921), *The Dynamic of Capillary Flow*, Phys. Rev. *17*, 273–283.

WINKLER, E. M., and SINGER, P. C. (1972), *Crystallization Pressure of Salts in Stone and Concrete*, Geol. Soc. Am. Bull. *83*, 3509–3514.

WYLIE, R. G., *The properties of salt-water systems in relation humidity*. In *Humidity and Moisture*, (Rheinhold Publ. Corp., New York 1963) *3*, pp. 507–517.

ZEHNDER, K. (1982), *Verwitterung von Molassesandsteinen an Bauwerken und in Naturaufschlüssen*, Beiträge z. Geologie d. Schweiz, Geotech. Kommission *61*, Kümmerly and Frey, Bern.

(Received October 31, 1994, accepted April 4, 1995)

List of Symbols

$\mathscr{A}$: weight increase by capillary imbibition
$\mathscr{B}$: capillary imbibition kinetic coefficient (experimental)
c: concentration in air
C: concentration in solution
$\mathscr{C}$: capillary imbibition kinetic coefficient ($=\mathscr{B}$)
$D(\theta)$: diffusivity
D_a: air dry diffusivity
D_i: initial diffusivity
$\mathscr{D}$: isothermal rate of diffusion for water vapour in air
h: distance of the meniscus from the evaporating end of the tube
k: water vapour conductivity in air
$K(\psi)$: hydraulic conductivity
K_0: saturated hydraulic conductivity
L: length of the sample, tube
N_l: porosity freely invaded in capillary imbibition
N_t: total porosity
M: molecular mass of water
$Q_{(0,\,t)}$: water balance at the surface of the rock
P: atmospheric pressure
p_0: saturated vapour pressure
p_1: fixed water pressure
q_c: capillary imbibition flow
q_e: evaporation flow
q_{ct}: constant rate of drying (massic)
q_v: constant rate of drying (volumic)
q^*: falling rate of drying
R: universal gas constant
r: hydraulic radius
S: macroscopical area through which water transfer occurs
S_{sa}: specific surface area
T: temperature
t: time
V: volume

x: distance of the meniscus from the evaporating end of the tube
x_0: initial distance of the meniscus from the evaporating end of the tube
y: height of the meniscus in a tube above the free water level
y_0: initial height of the meniscus
β: empirical constant
γ: surface tension
λ: thickness of the superficial concentrated layer
η: dynamic viscosity
ψ: matrix potential
θ: water content
θ_a: air-dry water content
θ_c: critical water content
θ_i: initial water content
ρ: fluid density
ε: thickness of the air layer over the water surface where $p_1 < p < p_0$